Small Molecule Activation and Capture by Preorganized Frustrated Lewis Pairs

Bertini, F.

2013

document version
Publisher's PDF, also known as Version of record

Chapter 4

Small Molecule Capture by P/Al-based Dimeric Lewis Pairs

Federica Bertini, Frank Hoffmann, Christian Appelt, Werner Uhl, Andreas W. Ehlers, J. Chris Slootweg, and Koop Lammertsma

Abstract: Methylene-bridged phosphinoalane $t\text{Bu}_2\text{PCH}_2\text{AlMe}_2$ exists as a stable, dimeric Lewis adduct, which reacts with carbon dioxide and *tert*-butyl isocyanate at room temperature, forming 5-membered heterocycles. The reaction pathways were explored with computational chemistry.

submitted to Organometallics

4.1. Introduction

Activation of small molecules to generate chemical building blocks is of fundamental importance and requires new strategies. Such is the case for the transformation of CO_2[1] and bio-renewable feedstock into useful chemicals. Traditionally, molecules like H_2, N_2, and CO_2 are activated by transition metals,[2] but the current focus on environmentally benign processes demands transition metal-free methodologies.[3] The recently discovered frustrated Lewis pairs (FLPs) fulfill this objective. FLPs are sterically encumbered combinations of Lewis acids and bases of main group elements that are inhibited from self-quenching. Instead they can cleave small molecules heterolytically.[4] By possessing a lone pair of electrons as well as a vacant orbital, FLPs mimic the properties of transition metals complexes. Even classical Lewis adducts can manifest FLP-type reactivity, be it with reduced activity owing to the energy needed to separate the Lewis acid and base components.[5] For example, adduct $Ph_3P{\rightarrow}B(C_6F_5)_3$ reacts with the C≡C triple bond of phenylacetylene despite the 39 kcal·mol^{-1} strong P–B bond;[5e] the weakly bonded P/B-intramolecular adduct $Mes_2PCH_2CH_2B(C_6F_5)_2$[5b] has been reacted with many substrates[6] and is a catalyst for the hydrogenation of organic molecules.[7]

Recently, we reported on the geminal P/Al-based FLP **A**[8,9] and its reactivity toward H_2, CO_2, alkynes, isocyanate, and alkali metal hydrides. Thereby we extended the chemistry of unimolecular FLPs to aluminum as Lewis acidic component. FLP **A** is pre-organized for small molecule capture since the C1-linker gives an ideal orientation of the Lewis acid and base centers.[9,8] The C1-linker has as additional advantage that it hampers intramolecular P→Al bond formation, and thus quenching of the reactive sites by formation of PCAl three-membered rings.[9]

Here we extend our approach to the C1-bridged P/Al-based Lewis pair tBu$_2$PCH$_2$AlMe$_2$ (**1**) and report on its ability to activate CO_2 and isocyanates. We were attracted to **1** because of its perceived facile synthesis from readily accessible tBu$_2$PCH$_2$Li[10] and commercially available ClAlMe$_2$.

We envisioned that the bulky *tert*-butyl substituents on phosphorus, in combination with the small methyl substituents on aluminum, might not provide sufficient steric shielding to prevent dimerization of **1**.[11] Nevertheless, we were encouraged by earlier reports on the reactivity of related $[R_2PCH_2AlR`_2]_2$ heterocycles, which suggested to us that dimeric [**1**]$_2$ might manifest FLP-type reactivity similar to **A**. For example, Karsch *et al*. reported that phosphinoalane $[Me_2PCH_2AlMe_2]_2$ (**B**) reacts with donor molecules such as PMe_3 and THF, causing dissociation of the dimer into Lewis base-stabilized monomeric units, while $[Me_2PCH_2AlCl_2]_2$ (**C**) was found to cleave THF to unidentified products.[12] More

recent studies showed **B** to act as co-catalyst in Si–Si bond formation (with (1-methyl-indenyl)Ni(Me)($Me_2PCH_2AlMe_2$) (**E**) being the intermediate)[13] and to react with Cp*$RhMe_2$(DMSO) to form Cp*$RhMe_2$($Me_2PCH_2AlMe_2$) (**F**), which is of interest in alkane activation.[14] Moreover, during our investigations Fontaine *et al*. reported on the reactivity of **B** toward CO_2.[15] These reports indicate that, despite their significant thermodynamic stability, dimeric [$R_2PCH_2AlR`_2$]$_2$ heterocycles posses an intriguing reactivity toward both nucleophiles and electrophiles.

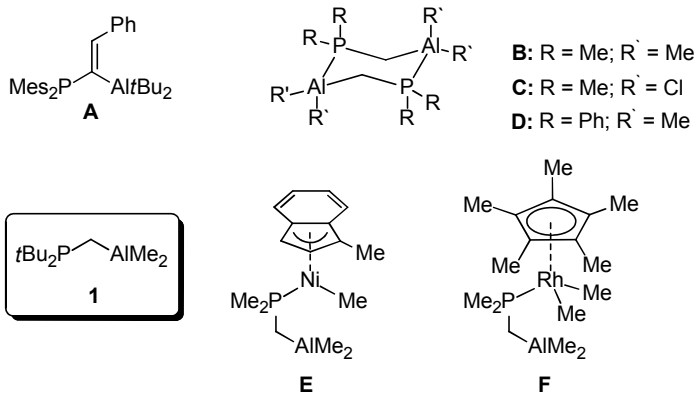

Scheme 1.

4.2. Results and Discussion

Salt metathesis of tBu_2PCH_2Li[10] with commercially available $ClAlMe_2$ (1M solution in hexanes) in methyl *tert*-butyl ether or diethyl ether gave the desired target [**1**]$_2$ as a colorless solid in 98% yield (δ^{31}P = 16.4 ppm). ^{1}H NMR spectroscopy (in C_6D_6) supported the dimeric nature of [**1**]$_2$ by showing a doublet of doublets for the methylene protons of the C1 linker (^2J(H,P) = 13.3 Hz, ^3J(H,P) = 4.6 Hz), due to different H,P couplings with the two phosphorus atoms, and coupling of the protons of the $AlMe_2$ group with the phosphorus atom directly bonded to aluminum (^3J(H,P) = 2.9 Hz).[12] Crystals suitable for single-crystal X-ray analysis were grown from a mixture of *c*-pentane and 1,2-difluorobenzene. The molecular structure confirmed the dimeric nature of [**1**]$_2$ and showed the six-membered heterocycle to adopt a chair conformation in the solid state (Figure 1).

The P–Al bond lengths (2.5001(5) Å) are typical for P–Al dative bonds, while the Al–CH_3 bond lengths (1.982(1) and 1.984(1) Å) are shorter than the Al–C distances for Al–CH_2–P (2.015(1) Å). [**1**]$_2$ crystallizes in the P21/c space group with a crystallographically imposed centrosymmetry, like that observed for **B**.[12]

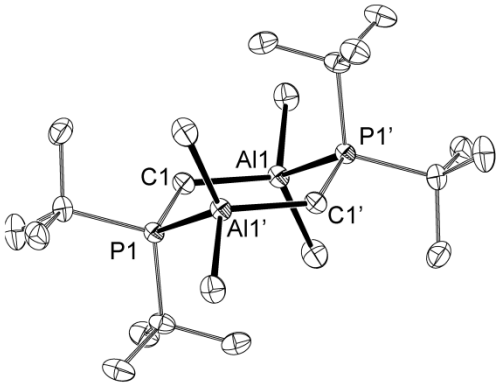

Figure 1. Molecular structure of [**1**]$_2$. Ellipsoids are set at 50% probability; H atoms have been omitted for clarity. Selected bond lengths [Å] and bond angles [°]: P(1)–Al(1)' 2.5001(5), P(1)−C(1) 1.805(1), Al(1)−C(1) 2.015(1), Al(1)−C(4) (equatorial) 1.984(1), Al(1)−C(5) (axial) 1.982(1), P(1)−C(3) (axial) 1.881(1), P(1)−C(2) (equatorial) 1.887(1), P(1)−C(1)−Al(1) 128.04(7), C(1)−Al(1)−P(1)' 102.4(4), Al(1)'−P(1)−C(1) 111.58(4).

The thermal stability of [**1**]$_2$ was examined with M06-2X/6-31+G(d,p)[16] theory for the full system (Figure 2). Throughout, Δ*G* energies are given for fully optimized geometries, unless noted otherwise. The calculations reveal a rather endergonic dissociation of [**1**]$_2$ into its monomeric *t*$Bu_2PCH_2AlMe_2$ units (30.6 kcal·mol^{-1}).[17] Only slightly less unfavorable is the single P–Al bond rupture (27.0 kcal·mol^{-1}) that leads to *open* chain [**1**]$_2^*$, which stabilizes on forming a Al–CH_3–Al 3c-2e bond to give [**1**]$_2^{**}$ (–4.7 kcal·mol^{-1}); the 'cost' of rupturing the second P–Al bond is modest (3.6 kcal·mol^{-1}). Monomeric **1** displays no intramolecular P–Al bonding interaction (3.19 Å) due to the perpendicularly positioned lone pair on phosphorus, but the ring-closed isomer **1*** (P–Al 2.60 Å; P–C–Al 84.9°) is nearly isoenergetic (1.1 kcal·mol^{-1}).

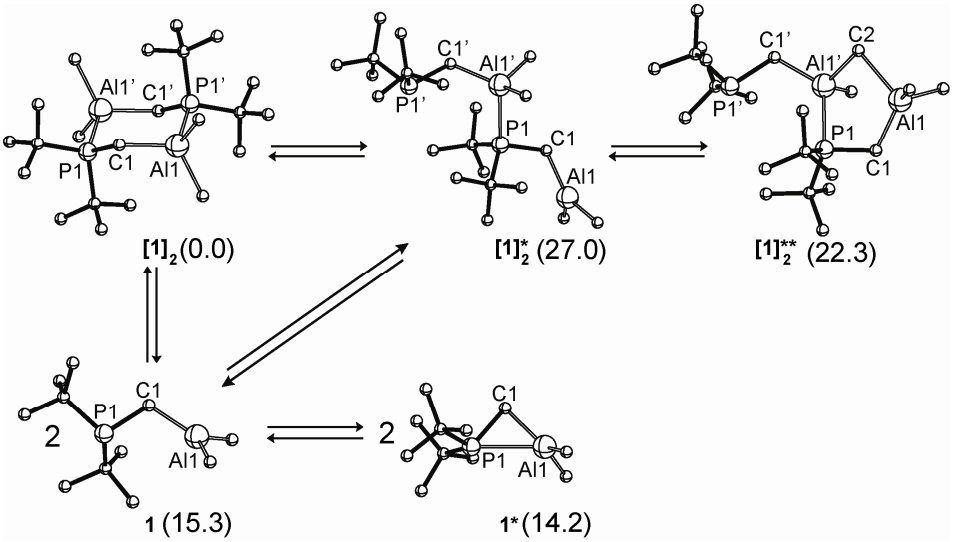

Figure 2. Computed structures for [**1**]$_2$, [**1**]$_2^*$, [**1**]$_2^{**}$, **1** and **1*** at the M06-2X/6-31+G(d,p) level of theory. The reported Gibbs free energies are in kcal·mol^{-1} of dimer, except for the interconversion of **1** into **1*** (here we refer to a mole of monomer). Selected bond lengths [Å] and angles [°] for: [**1**]$_2$: P1–C1 1.820, C1–Al1 2.033, Al1–P1` 2.514; P1–C1–Al1 125.3. [**1**]$_2^*$: P1–C1 1.847, C1–Al1 1.986, P1'–C1' 1.851, C1'–Al1' 2.011, Al1'–P1 2.561. [**1**]$_2^{**}$: P1–C1 1.184, C1–Al1 2.023, Al1–C2 2.292, P1'–C1' 1.852, C1'–Al1' 1.998, Al1'–P1 2.475; Al1'–C2–Al1 92.6. **1**: P1–C1 1.851, Al1–C1 1.970, P1–Al1 3.188; P1–C1–Al1 113.1. **1***: P1–C1 1.863, Al1–C1 1.982, P1–Al1 2.597; P1–C1–Al1 84.9.

Despite the apparent thermal stability of the dimer [**1**]$_2$, we were eager to explore its reactivity. In the presence of THF, [**1**]$_2$ partially dissociates at room temperature to give a mixture of [**1**]$_2$ (δ^{31}P = 16.4) and **1-THF** (δ^{31}P = 27.7). Monitoring of a 3:1 mixture of D_8-toluene/THF solution by ^{31}P NMR at various temperatures confirmed the equilibrium with the concentration of [**1**]$_2$ increasing upon cooling, leading to a ~1:1 ratio at –63 °C. Whereas the ^{1}H NMR resonances of the coordinated THF molecules of **1-THF** are not distinguishable from those of uncoordinated THF, fragmentation of the dimer is evident from the loss of the characteristic ^3J(H,P) couplings for the PCH_2Al and Al(CH_3)$_2$ hydrogens.

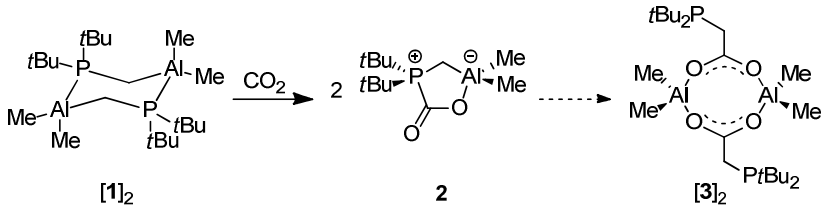

Scheme 2. CO_2 uptake by [**1**]$_2$ to give CO_2-adduct **2** and conversion of **2** into [**3**]$_2$.

Having established that [**1**]$_2$ dissociates in THF, we decided to explore its reactivity toward CO_2. Encouraged by the M06-2X/6-31+G(d,p) calculations that showed the reaction with CO_2 (2 equiv) to be exergonic by 10.7 kcal·mol^{-1}, we found a suspension of [**1**]$_2$ in toluene to react rapidly with CO_2 at ambient conditions to a single product (**2**), which was isolated as a colorless oil in 77% yield (δ^{31}P = 50.7; Scheme 2). Its ^{13}C NMR spectrum showed a characteristic doublet (δ^{13}C = 167.6 ppm, ^1J(C,P) = 94.1 Hz) for the CO_2-adduct. Samples of **2** proved to be thermally stable, even when heated in C_6D_6 at 70 °C for 14 h. Computations confirm this stability, namely decomposition requires 45.2 kcal·mol^{-1} by splitting the P–C bond first, giving van der Waals complex **vdW** ($\Delta G^{\ddagger}$ = 23.6 (**TS1**), ΔG = 22.3 kcal·mol^{-1}),[8] followed by rearrangement to carboxylate **3** ($\Delta G^{\ddagger}$ = 45.2 (**TS2**), ΔG = –9.7 kcal·mol^{-1}; Figure 3).[18] Nevertheless, dimer [**3**]$_2$ (δ^{31}P = 37.8; δ^{13}C = 184.1, ^2J(C,P) = 15.2 Hz) has been obtained from **2** in select cases (Scheme 2)[19] and in the similar rearrangement of the Me_2P-analogue **B**-CO_2, reported by Fontaine *et al.* (see also Figure 3).[15] However, given the high reaction barriers, we presume that unidentified impurities act as catalyst in these reactions. Further investigations are in progress.

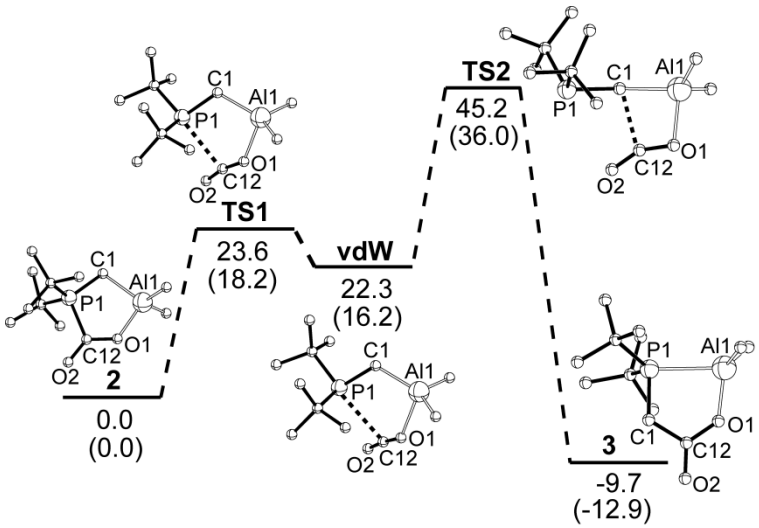

Figure 3. Relative M06-2X/6-31+G(d,p) Gibbs free energies (in kcal·mol^{-1}) for the rearrangement of **2** into **3**. Values in parentheses refer to the analogous rearrangement of the **B**-CO_2 adduct. Selected bond lengths [Å] and angles [°] for **2**: P1−C1 1.78, P1−C12 1.90, Al1−O1 1.88, Al1−C1 2.08, C12−O1 1.28, C12−O2 1.21. **TS1**: P1−C1 1.84, P1−C12 2.88, Al1−O1 2.17, Al1−C1 2.00, C12−O1 1.18, C12−O2 1.16. **vdW**: P1−C1 1.85, P1−C12 3.07, Al1−O1 2.27, Al1−C1 1.99. **TS2**: P1−C1 1.86, C1−Al1 2.08, Al1−O1 1.96, C12−O1 1.22, C12−O2 1.16, C12−C1 2.28. **3**: P1−Al1 2.53, P1−C1 2.53, O1−Al1 1.81, C1−C12 1.54, C12−O1 1.31, C12−O2 1.21.

In spite of the exergonicity (10.7 kcal·mol^{-1}), the CO_2 uptake by dimer [**1**]$_2$ is remarkable because of its highly unfavorable dissociation into reactive monomers (30.5 kcal·mol^{-1}). Moreover, CO_2-adduct **2** is formed in apolar toluene, whereas other Lewis adducts (e.g., $Ph_3P{\rightarrow}B(C_6F_5)_3$)[5e] react in polar solvents (e.g., chlorobenzene) that promote solvent-assisted frustration.[20] The question arises, whether the CO_2 substrate can induce frustration in the present case. We tested this hypothesis with M06-2X/6-31+G(d,p) calculations. In the geometry optimized van der Waals CO_2-[**1**]$_2$ adduct **4** (Figure 4), formed from its constituents (ΔG = 6.5, ΔE = −2.8 kcal·mol^{-1}), the almost linear CO_2 fragment (179.5°) is only modestly attracted to [**1**]$_2$ (d(Al–O) 3.523 Å); the Al–P bond (2.518 Å) is of normal length. Al–O shortening causes the P–Al bond to rupture with simultaneous formation of ring-opened FLP **5** (Al–O 2.784, Al–P 3,830 Å; Figure 4). Whereas the formal dissociation of [**1**]$_2$, remains energetically demanding, the beneficiary effect of a single CO_2 molecule is evident (ΔG = 27.5, ΔE = 21.2 kcal·mol^{-1}). It is

reasonable to assume that additional CO_2 (and solvent) molecules may provide additional stabilization.

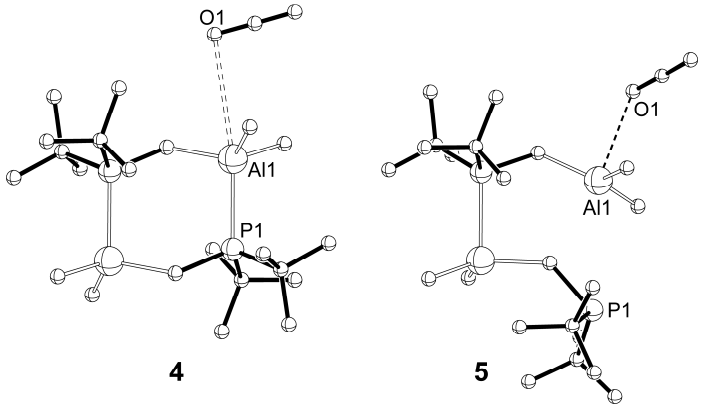

Figure 4. CO_2-adducts **4** and **5** of dimeric Lewis pair [**1**]$_2$.

The facile CO_2 uptake prompted us to investigate the reactivity of [**1**]$_2$ toward *tert*-butyl isocyanate. FLPs are known to react with isocyanates by selective 1,2-cycloaddition to either the C=O[9,21] or C=N bond.[22] An M06-2X/6-31+G(d,p) survey confirmed the exergonicity of this reaction and suggested that [**1**]$_2$ would favor P/Al addition to the C=N bond of the isocyanate over that to the C=O double bond (–25.2 *vs* –18.0 kcal·mol^{-1}) in line with experiments. Thus, treating [**1**]$_2$ with *t*BuNCO (6.4 equiv) in toluene at room temperature led indeed to the selective formation of C=N adduct **6** (δ^{31}P = 41.4), which was isolated as a colorless solid in 61% yield (Figure 5). A single-crystal X-ray analysis confirmed the formation of **6**. Its molecular structure (Figure 5) displays an almost planar 5-membered PC_2AlN heterocycle with a rather short endocyclic C–N bond (1.334(2) Å), an elongated exocyclic C–O bond (1.236(2) Å), and a planar nitrogen atom (sum of angles 359.9°), all of which underscore the contribution of resonance structure **6'** (Figure 5). Characteristic signals for the carbonyl group are observed in the IR spectrum (stretch 1600 cm^{-1}) and in the ^{13}C NMR spectrum as a doublet (δ^{13}C = 168.2 ppm; ^1J(C,P) = 101.9 Hz).

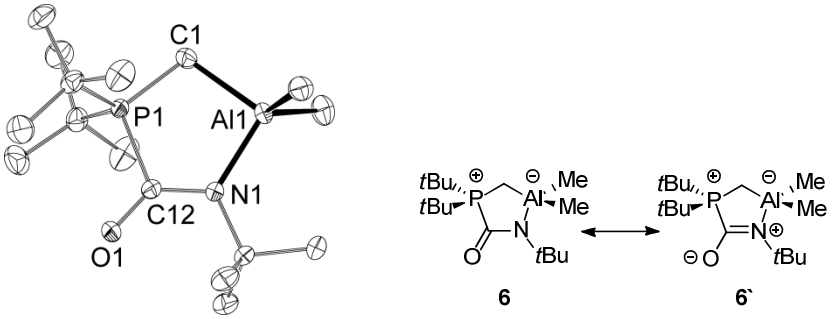

Figure 5. Molecular structure of **6**. Ellipsoids are set at 50% probability; H atoms have been omitted for clarity. Selected bond lengths [Å] and bond angles [°]: P(1)–C(12) 1.866(1), C(12)–N(1) 1.334(2), N(1)–Al(1) 1.947(1), Al(1)–C(1) 2.045(2), P(1)–C(1) 1.764(1), C(12)–O(1) 1.236(2), P(1)–C(1)–Al(1) 105.27(7), C(1)–P(1)–C(12) 106.73(7), C(1)–Al(1)–N(1) 94.71(5), P(1)–C(12)–N(1) 113.2(1), C(12)–N(1)–C(13) (*t*Bu) 116.8(1), Al(1)–N(1)–C(13) (*t*Bu) 123.64(9), C(12)–N(1)–Al(1) 119.41(9).

4.3. Conclusions

In this study, the chemistry of geminal FLPs has been extended to readily available, P/Al-based classical Lewis adduct [**1**]$_2$. We have demonstrated that such stable dimers are quite reactive toward small oxygen (THF and CO_2) and nitrogen (*t*BuNCO) donors by substrate-induced frustration.

4.4. Computational Section

General. The computational study was performed using Gaussian 09 suite of programs (Revision A.02).[23] All DFT calculations were conducted using the dispersion-corrected functional M06-2X and 6-31+G(d,p) basis set.[16] Frequency calculations on the computed structures confirmed the nature of the computed minima and transition states and allowed ZPE corrections on the computed energies. The computed energies reported in this work refer to the molecules in the gas phase. The computed electronic energies (E), zero point energies (ZPE) and Gibbs free energies (G) are given in atomic units. Relative energies (ΔE, ΔE(ZPE) and ΔG) are given in kcal·mol^{-1}.

4.4.1. Structural Analysis of $[\mathbf{1}]_2$

We performed a computational analysis to investigate on the stability of dimer $[\mathbf{1}]_2$. The energies of the computed structures, which are shown in Figure 2 (Section 4.2), are reported in Table 1. Thermal corrections to enthalpy, thermal corrections to Gibbs free energy and total entropy of the computed structures are listed in Table 2.

	E	ΔE	ZPE	ΔE(ZPE)	G	ΔG
$[\mathbf{1}]_2$	-2036.821298	0.0	0.698158	0.0	-2036.187570	0.0
$[\mathbf{1}]_2$[(a)]	-2036.816385	3.1	0.698676	3.4	-2036.181744	3.7
$[\mathbf{1}]^*_2$	-2036.771353	31.3	0.695934	29.9	-2036.144558	27.0
$[\mathbf{1}]^{**}_2$	-2036.783616	23.6	0.697684	23.3	-2036.151994	22.3
1	-1018.368068	26.7[(b)]	0.345941	24.8[(b)]	-1018.069449	15.3[(b)]
1*	-1018.368305	26.6[(b)]	0.346773	25.1[(b)]	-1018.068164	14.2[(b)]

Table 1. M06-2X/6-31+G(d,p) energies of the computed structures. (a) Dimer $[\mathbf{1}]_2$ in the twisted boat conformation. (b) Such relative energies refer to 1 mole of monomer (**1** or **1***), relatively to 0.5 moles of dimer in the chair conformation ($[\mathbf{1}]_2$).

	Hcorr	Stot	Gcorr
$[\mathbf{1}]_2$	0.739237	222.064	0.633727
$[\mathbf{1}]_2$[(a)]	0.739710	221.137	0.634640
$[\mathbf{1}]^*_2$	0.737990	234.028	0.626795
$[\mathbf{1}]^{**}_2$	0.738972	225.936	0.631622
1	0.367379	144.718	0.298619
1*	0.368054	142.935	0.300142

Table 2. M06-2X/6-31+G(d,p) thermal corrections to enthalpy (a.u.), thermal corrections to Gibbs free energy (a.u.) and total entropy (cal/mol·K) for the computed structures. (a) Dimer $[\mathbf{1}]_2$ in the twisted boat conformation.

4.4.2. Reaction of $[1]_2$ with CO_2

We performed a computational analysis to investigate on the reaction of **1** (monomer) with CO_2. We could locate, on the PES (potential energy surface), structures **vdW** and **2** as energy minima, and **TS1** as a transition state connecting **vdW** to **2** (see Figure 3, Section 4.2). The formation of **1** from 0.5 moles of $[\mathbf{1}]_2$ is endoergonic (ΔG = 15.3 kcal·mol^{-1}; Table 1). The computed energies for the reaction of **1** with CO_2 are reported in Table 3. Thermal corrections to enthalpy, thermal corrections to Gibbs free energy and total entropy of the computed structures are listed in Table 4.

	E	Δ*E*	ZPE	Δ*E*(ZPE)	G	Δ*G*
1	-1018.368068	–	0.345941	–	-1018.069449	–
CO_2	-188.516053	–	0.011930	–	-188.524817	–
vdW	-1206.896520	-7.8	0.359351	-6.9	-1206.591653	1.6
TS1	-1206.896302	-7.6	0.358744	-7.1	-1206.589555	3.0
2	-1206.939024	-34.5	0.361508	-32.2	-1206.627119	-20.6

Table 3. M06-2X/6-31+G(d,p) energies of the computed structures.

	Hcorr	Stot	Gcorr
1	0.367379	144.718	0.298619
CO_2	0.015487	51.040	-0.008764
vdW	0.384542	167.690	0.304867
TS1	0.383165	160.833	0.306748
2	0.385244	154.354	0.311905

Table 4. M06-2X/6-31+G(d,p) thermal corrections to enthalpy (a.u.), thermal corrections to Gibbs free energy (a.u.) and total entropy (cal/mol·K) for the computed structures.

4.4.3. Rearrangement of CO_2 Adducts

In order to rationalize the unexpected rearrangement of **2** into **3**, which we have observed in select cases, and which was also observed by Fontaine and co-workers for the CO_2-adducts of **B** and **D**, we resorted again to computational chemistry.

First, we computed the reaction pathway proposed by Fontaine *et al.*[15] for the rearrangement of $Me_2PCH_2AlMe_2$–CO_2 adduct (**B**-CO_2) into the Al-carboxylate **3B** (analogous to **3**; Figure 3, Section 4.2) at M06-2X/6-31+G(d,p) level of theory. This allowed comparison of our results with the ones obtained by Fontaine *et al.* using the B3LYP functional and 6-31+G(d,p) basis set.[15] The computed reaction pathway is analogous to the one shown for the rearrangement of **2** (into **3**) in Figure 3 (Section 4.2). The relative SCF energies and Gibbs free energies for the computed structures using the

two different functionals are reported in Table 5. We observed deviations in the computed relative energies within ±3 kcal·mol^{-1}. We note that the overall barrier predicted using the M06-2X functional (36.0 kcal·mol^{-1}) is even higher than the one predicted by B3LYP (34.7 kcal·mol^{-1}). We point out that such high reaction barriers contrast with the facile rearrangement observed experimentally. In fact, the complete rearrangement of **B**-CO_2 was observed to occur in 1h at room temperature, while it was complete after only 10 minutes with **D**-CO_2, for which a similar barriers were predicted.[15]

	Δ*E* (B3LYP)	**Δ*E* (M06-2X)**	**Δ*G* (B3LYP)**	**Δ*G* (M06-2X)**
B-CO_2	0.0	0.0	0.0	0.0
TS1-B	18.7	21.6	16.1	18.2
vdW-B	18.4	20.4	14.8	16.2
TS2-B	36.8	38.8	34.7	36.0
3B	-12.2	-12.7	-11.1	-12.9
[**3B**]$_2$	-35.6	-38.6	-28.7	-30.7

Table 5. Comparison between the computed relative SCF energies (non ZPE corrected) and Gibbs free energies of the computed structures (in kcal·mol^{-1}), which were optimized at B3LYP/6-31+G(d,p) and M06-2X/6-31+G(d,p) level of theory.

	E	**Δ*E***	**ZPE**	**Δ*E*(ZPE)**	**G**	**Δ*G***
B-CO_2	-971.161601	0.0	0.189703	0.0	-971.012362	0.0
TS1-B	-971.127142	21.6	0.187685	20.4	-970.983316	18.2
vdW-B	-971.129031	20.4	0.187979	19.4	-970.986560	16.2
TS2-B	-971.099695	38.8	0.187924	37.7	-970.954962	36.0
3B	-971.181908	-12.7	0.189703	-11.7	-971.012362	-12.9
[**3B**]$_2$	-1942.446273	-38.6	0.386470	-36.4	-1942.122585	-30.7

Table 6. M06-2X/6-31+G(d,p) energies of the computed structures.

	Hcorr	**Stot**	**Gcorr**
B-CO_2	0.205109	117.588	0.149239
TS1-B	0.204375	127.437	0.143826
vdW-B	0.205618	132.904	0.142471
TS2-B	0.204239	125.241	0.144733
3B	0.207680	123.651	0.148929
[**3B**]$_2$	0.417843	198.167	0.323687

Table 7. M06-2X/6-31+G(d,p) thermal corrections to enthalpy (a.u.), thermal corrections to Gibbs free energy (a.u.) and total entropy (cal/mol·K) for the computed structures.

Next, we computed the analogous reaction pathway for the rearrangement of *t*$Bu_2PCH_2AlMe_2$–CO_2 adduct **2** into **3** (Figure 3, Section 4.2), and finally [**3**]$_2$. We note that with *tert*-butyl substituents on phosphorus (instead of Me or Ph) the CO_2 uptake is far more exothermic. Consequently, the reverse reaction, namely the dissociation of CO_2 from **2** to give **vdW** occurs with a significantly higher barrier (23.6 kcal·mol^{-1} for **2** *vs* 16.2 kcal·mol^{-1} for **B**-CO_2). The overall barrier for such rearrangement is of 45.2 kcal·mol^{-1}, which leads to the conclusion that the rearrangement cannot occur at room temperature *via* this mechanism. This is in agreement with the thermal stability observed for some samples of **2**, which resulted stable towards rearrangement even upon heating (as described in Section 4.2). The computed energies are reported in Table 8. Thermal corrections to enthalpy, thermal corrections to Gibbs free energy and total entropy of the computed structures are listed in Table 9.

	E	Δ*E*	ZPE	Δ*E*(ZPE)	G	Δ*G*
2	-1206.939024	0.0	0.361508	0.0	-1206.627119	0.0
TS1	-1206.896302	26.8	0.358744	25.1	-1206.589555	23.6
vdW	-1206.896520	26.7	0.359351	25.3	-1206.591653	22.3
TS2	-1206.864624	46.7	0.359534	45.4	-1206.555072	45.2
3	-1206.957927	-11.9	0.363694	-10.5	-1206.642561	-9.7
[**3**]$_2$	-2413.976699	-31.0	0.730053	-28.7	-2413.319897	-20.6

Table 8. M06-2X/6-31+G(d,p) energies of the computed structures.

	Hcorr	Stot	Gcorr
2	0.385244	154.354	0.311905
TS1	0.383165	160.833	0.306748
vdW	0.384542	167.690	0.304867
TS2	0.383338	155.294	0.309552
3	0.387032	150.833	0.315366
[**3**]$_2$	0.775863	250.583	0.656803

Table 9. M06-2X/6-31+G(d,p) thermal corrections to enthalpy (a.u.), thermal corrections to Gibbs free energy (a.u.) and total entropy (cal/mol·K) for the computed structures.

4.4.4. Reaction of [1]$_2$ with *t*BuNCO

To gain a deeper understanding of the exclusive formation of **6** from the reaction of [**1**]$_2$ with *t*BuNCO, we computed the structures of all possible products that could result from P/Al addition to either the C=O or the C=N bond of *t*BuNCO, namely *Z*-**6**$_{\mathbf{C=O}}$, *E*-**6**$_{\mathbf{C=O}}$ and **6** (Figure 6). Formation of *Z*-**6**$_{\mathbf{C=O}}$ from [**1**]$_2$ is energetically unfavored (Δ*G* = 20.3

kcal·mol^{-1}), probably as a consequence of steric repulsion between the bulky *tert*-butyl substituent on the nitrogen atom of the isocyanate and the *tert*-butyl substituents on the phosphorus atom, while the formation of products *E*-**6**$_{\mathbf{C=O}}$ (ΔG = -9.0 kcal·mol^{-1}) and **6** (ΔG = -12.6 kcal·mol^{-1}) from [**1**]$_2$ is energetically favored, with **6** being the most stable product.

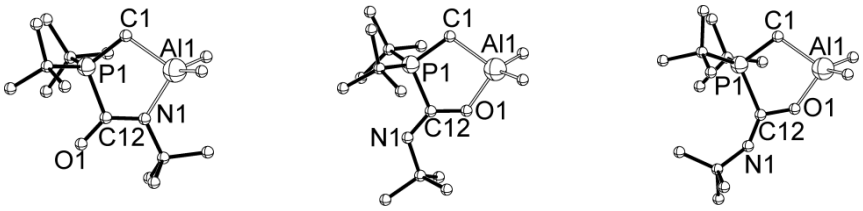

6 *E*-**6**$_{C=O}$ *Z*-**6**$_{C=O}$

Figure 6.

The relative energies reported in Table 10 refer to the reaction of 1 isocyanate molecules with half a molecule of [**1**]$_2$. Thermal corrections to enthalpy, thermal corrections to Gibbs free energy and total entropy of the computed structures are listed in Table 11.

	E	Δ*E*	ZPE	Δ*E*(ZPE$_{corr}$)	G	Δ*G*
½ [**1**]$_2$	-1018.408192	–	0.399338	–	-1018.093785	–
***t*BuNCO**	-325.804863	–	0.135757	–	-325.70	–
6	-1344.248326	-22.1	0.486737	-21.1	-1343.82	-12.6
E-**6**$_{C=O}$	-1344.242265	-18.3	0.485775	-17.9	-1343.81	-9.0
Z-**6**$_{C=O}$	-1344.195588	11.0	0.485573	11.3	-1343.77	20.3

Table 10. M06-2X/6-31+G(d,p) energies of the computed structures.

	Hcorr	Stot	Gcorr
½ [**1**]$_2$	0.369619	111.032	0.316864
***t*BuNCO**	0.145001	92.161	0.101212
6	0.515925	179.129	0.430816
E-**6**$_{C=O}$	0.514553	176.879	0.430512
Z-**6**$_{C=O}$	0.515102	178.072	0.430494

Table 11. M06-2X/6-31+G(d,p) thermal corrections to enthalpy (a.u.), thermal corrections to Gibbs free energy (a.u.) and total entropy (cal/mol·K) for the computed structures.

4.4.5. Substrate Assisted Frustration

We have explained in Section 4.2 that we have considered the possibility that the substrate (CO_2) induces frustration by promoting the cleavage of the P–Al bond in [**1**]$_2$. To test this hypothesis, we calculated two CO_2-adducts (**4** and **5**, shown in Figure 4, Section 4.2) of [**1**]$_2$ at the M06-2X/6-31+G(d,p) level of theory. The computed energies are reported in Tables 12. Thermal corrections to enthalpy, thermal corrections to Gibbs free energy and total entropy of the computed structures are listed in Table 13.

	E	Δ*E*	ZPE	Δ*E*(ZPE)	G	Δ*G*
[**1**]$_2$	-2036.821298	–	0.698158	–	-2036.187570	–
CO_2	-188.516053	–	0.011930	–	-188.52	–
4	-2225.341813	-2.8	0.711095	-2.2	-2224.701982	6.5
5	-2225.303509	21.2	0.709663	21.0	-2224.668514	27.5

Table 12. M06-2X/6-31+G(d,p) energies of the computed structures.

	Hcorr	Stot	Gcorr
[**1**]$_2$	0.739237	222.064	0.633727
CO_2	0.015487	51.040	-0.008764
4	0.755616	243.690	0.639831
5	0.755540	253.707	0.634995

Table 13. M06-2X/6-31+G(d,p) thermal corrections to enthalpy (a.u.), thermal corrections to Gibbs free energy (a.u.) and total entropy (cal/mol·K) for the computed structures.

4.5. Experimental Section

General. All syntheses were performed with the use of Schlenk techniques under an atmosphere of dry nitrogen. All solvents were freshly distilled and stored over a sodium mirror. NMR spectra were recorded at 300.2 K on a Bruker Avance 500 (^{1}H, ^{13}C) or a Bruker Avance 400 (^{1}H, ^{13}C, ^{31}P, ^{11}B) and referenced internally to residual solvent resonances. IR spectra were recorded on a Shimadzu FTIR–8400S spectrophotometer. Fast Atom Bombardment (FAB) mass spectrometry was carried out using a JEOL JMS SX/SX 102A four-sector mass specrometer, coupled to a JEOL MS-MP9021D/UPD system program. Samples were loaded in a matrix solution (3-nitrobenzyl alcohol) on to a stainless steel probe and bombarded with Xenon atoms with an energy of 3KeV. During the high resolution FAB-MS measurements a resolving power of 10,000 (10% valley definition) was used. Melting points were measured on samples in sealed capillaries and are uncorrected. *t*Bu$_2$PCH$_2$Li was synthesized according to literature procedures.[10] ClAlMe$_2$ was purchased from Sigma-Aldrich as a 1M solution in hexane. Dry CO_2 was generated from dry ice which was allowed to sublime at room temperature and passed through concentrated sulfuric acid and P_2O_5. Commercially available *tert*-butyl isocyanate was distilled over CaH_2.

Synthesis of [1]$_2$. *t*Bu$_2$PCH$_2$Li (5 mmol, 0.83 g) was suspended in dry methyl *tert*-butyl ether (40 mL) and the resulting mixture was cooled to –78 °C. A 1M solution of ClAlMe$_2$ (5 mL, 5 mmol) in hexanes was added to the suspension and the reaction mixture was stirred for 30 min at –78 °C and then allowed to warm to room temperature and stirred overnight. The solution was filtered *via* a cannula into another flame-dried Schlenk vessel to remove LiCl. The ^{31}P{^{1}H} NMR spectrum of the crude mixture showed the formation of a single product with a singlet at δ = 16.4. Removal of all volatiles under reduced pressure yielded a colorless solid (Yield: 1.06 g, 4.9 mmol, 98%). Alternatively, in a 10 mmol scale reaction, the reaction mixture after filtration was stored at –20 °C affording colorless crystals (Yield: 1.30 g, 6.0 mmol, 60%). M.p. 250 °C. ^{31}P NMR (162.0 MHz, C_6D_6): δ 16.4. ^{1}H NMR (500.2 MHz, C_6D_6): δ –0.15 (d, $^{3}J_{HP}$ = 2.9 Hz, 12H; Al(CH_3)$_2$), 0.27 (dd, $^{2}J_{HP}$ = 13.3 Hz, $^{3}J_{HP}$ = 4.5 Hz, 4H; PCH_2Al), 1.13 (d, $^{3}J_{HP}$ = 12.5 Hz, 36H; P(C(CH_3)$_3$)$_2$). ^{13}C{^{1}H} NMR (125.8 MHz, C_6D_6): δ –2.7 (br. s; Al(CH_3)$_2$), –1.6 (br. s; PCH$_2$Al), 28.6 (d, $^{2}J_{CP}$ = 4.2 Hz; P(C(CH_3)$_3$)$_2$), 32.9 (d, $^{1}J_{CP}$ = 13.7 Hz; P(C(CH$_3$)$_3$)$_2$). HR-FABMS: calcd for $C_{22}H_{53}P_2Al_2$ [M+H]$^+$: 433.3253, found: 433.3255; *m/z* (%): 433 (3) [M+H]$^+$, 393 (12), 377 [M–*t*Bu]$^+$, 359 (44), 275 (30), 217 (20) [M/2+H]$^+$, 177 (100), 57 (50) [*t*Bu]$^+$.

Reaction of [1]$_2$ with THF. A spatula tip of [**1**]$_2$ (about 10 mg) was dissolved in 0.5 mL of C_6D_6 in an NMR tube and two drops of dry THF were added. The resulting mixture was analyzed by multinuclear NMR, which showed a 1:1 mixture of dimeric [**1**]$_2$ and **1-THF**. (3 : 1 mixture of D_8-toluene and THF was used for the low temperature NMR experiments). NMR data for **1-THF** at ambient temperature: $^{31}P\{^1H\}$ NMR (162.0 MHz, C_6D_6): δ 27.7. ^1H NMR (500.2 MHz, C_6D_6): δ −0.40 (s, 6H; Al(CH_3)$_2$), 0.01 (br. d, $^2J_{HP}$ = 1.3 Hz, 2H; PCH_2Al), 1.26 (d, $^3J_{HP}$ = 10.0 Hz, 18H; P(C(CH_3)$_3$)$_2$). $^{13}C\{^1H\}$ NMR (125.8 MHz, C_6D_6): δ −8.0 (br. s; Al(CH$_3$)$_2$), −0.1 (br. s; PCH$_2$Al), 29.9 (d, $^2J_{CP}$ = 14.3 Hz; P(C(CH$_3$)$_3$)$_2$), 31.3 (d, $^1J_{CP}$ = 26.3 Hz, P($\underline{C}$(CH$_3$)$_3$)$_2$). Coordinated THF could not be distinguished from free THF in the mixture, due to rapid solvent exchange.

Reaction of [1]$_2$ with CO_2. Synthesis of 2: [**1**]$_2$ (199 mg, 0.46 mmol) was suspended in toluene (15 mL) and (dry) CO_2 was bubbled through the solution for 10 minutes at room temperature and atmosphere pressure until a clear solution was formed. All volatiles were removed under vacuum yielding **2** as a colorless oil in 77 % yield (184 mg, 0.71 mmol). $^{31}P\{^1H\}$ NMR (161.9 MHz, C_6D_6): δ 50.6. ^1H NMR (400.0 MHz, C_6D_6): δ −0.37 (s, 6H; Al(CH_3)$_2$), 0.02 (d, ^2J(H,P) = 12.4 Hz, 2H; PCH_2Al), 0.96 (d, ^3J(H,P) = 14.9 Hz, 18H; P(C(CH_3)$_3$)$_2$). $^{13}C\{^1H\}$ NMR (100.6 MHz, C_6D_6): δ −8.5 (s; Al(CH$_3$)$_2$), −8.4 (d, ^1J(C,P) = 19.9 Hz; PCH$_2$Al), 26.7 (s; P(C(CH$_3$)$_3$)$_2$), 33.3 (d, ^1J(C,P) = 29.6 Hz; P(C(CH$_3$)$_3$)$_2$), 167.6 (d, ^1J(C,P) = 94.1 Hz; PC(O)OAl). MS (EI, 20 eV, 313 K) *m/z* (%): 177 (9), 161 (5), 160 (45), 137 (47), 136 (5), 120 (41), 105 (5), 104 (54), 97 (9), 94 (6), 80 (8), 78 (10), 58 (6), 57 (100), 56 (7). IR (CsI plates, paraffin): 1694 vs, 1607 s, 1568 vs ν(CO); 1466 vs, 1375 vs (paraffin); 1306 m, 1254 s δ(CH$_3$); 1188 s, 1146 w, 1080 w, 1020 s, 964 w, 916 s, 868 w, 841 w, 822 m, 812 m, 797 m ν(CC), ν(CO); 721 vs (paraffin); 694 s, 683 m, 665 m, 584 m, 540 w, 463 s ν(AlC), ν(PC), δ(CC).

Rearrangement of 2 into [3]$_2$: 0.5 mmol of spectroscopically pure, crystalline [**1**]$_2$ was suspended in dry toluene (30 mL) and CO_2 was subsequently bubbled into the suspension until a clear solution was obtained (*circa* 20 seconds). $^{31}P\{^1H\}$ NMR analysis of the crude reaction mixture revealed the formation of **2**. Monitoring the reaction by multinuclear NMR (in D-toluene) revealed the clean rearrangement of **2** into [**3**]$_2$: $^{31}P\{^1H\}$ NMR (162.0 MHz, RT, D_6-toluene): δ 37.8. ^1H NMR (400.1 MHz, RT, D_6-toluene): −0.32 (s, 6H; Al(CH_3)$_2$), 0.95 (d, ^3J(H,P) = 11.4 Hz, 36H; P(C(CH_3)$_3$)$_2$, 2.16 (d, ^2J(H,P) = 1.2 Hz, 4H; PCH_2). $^{13}C\{^1H\}$ NMR (125.8 MHz, RT, D_6-toluene): δ −10.7 (s; Al(CH$_3$)$_2$), 29.2 (d, ^2J(C,P) = 15.2 Hz; P(C(CH$_3$)$_3$)$_2$), 32.1 (d, ^1J(C,P) = 25.6 Hz; P(C(CH$_3$)$_3$)$_2$), 31.9 (d, ^1J(C,P) = 34.7 Hz; PCH$_2$), 184.06 (d, ^2J(C,P) = 15.2 Hz; P(CH$_2$)C(O)OAl).

Reaction of [1]$_2$ with *t*BuNCO. Synthesis of 6. [**1**]$_2$ (0.24 g, 0.55 mmol) was dissolved toluene (2 mL) and 0.4 mL of *t*BuNCO (0.35 g, 3.5 mmol) was added at room temperature. The reaction mixture was left to stir for 19h, after which all volatiles were removed under vacuum. Analysis of the crude product by ^{1}H NMR spectroscopy showed the selective formation of a single product, which was washed with pentane (1.5 mL), and dried under vacuum. (Yield: 0.21 g, 0.67 mmol, 61%). M.p. 141.8 °C. ^{31}P{^{1}H} NMR (162.0 MHz, C_6D_6): δ 41.4. ^{15}N{^{1}H} NMR (50.7 MHz, C_6D_6): δ 193 ppm. ^{1}H NMR (500.2 MHz, C_6D_6): δ –0.20 (s, 6H; Al(CH_3)$_2$), –0.16 (d, ^2J(H,P) = 12.9 Hz, 2H; PCH_2Al), 1.00 (d, ^3J(H,P) = 14.2 Hz, 18H; P(C(CH_3)$_3$)$_2$), 1.66 (d, ^5J(H,P) = 0.8 Hz, 9H; N(C(CH_3)$_3$)$_2$). ^{13}C{^{1}H} NMR (125.8 MHz, C_6D_6): δ –4.8 (br. s; Al(*C*H$_3$)$_2$), –10.7 (d, ^1J(C,P) = 13.5 Hz; P*C*H$_2$Al), 26.8 (s; P(C(*C*H$_3$)$_3$)$_2$), 29.2 (s; N(C(*C*H$_3$)$_3$)$_2$), 33.1 (d, ^1J(C,P) = 32.4 Hz; P(*C*(CH$_3$)$_3$)$_2$), 56.0 (d, ^3J(C,P) = 10.5 Hz; N(*C*(CH$_3$)$_3$)$_2$, 168.2 (d, ^1J(C,P) = 101.9 Hz; P*C*O). The signal at –10.7 ppm was observed in the ^{13}C{^{1}H} NMR spectrum as a broad singlet; the ^1J(C,P) was derived from the HSQC spectrum. IR: 1600 cm^{-1}. HR-FABMS: calcd for $C_{16}H_{36}ONPAl$ [M+H]$^+$: 316.2350, found: 316.2357; *m/z* (%): 316 (5) [M+H]$^+$, 300 (100), 260 (78) [M+2H-*t*Bu]$^+$, 233 (30), 217 (5) [*t*Bu$_2$OCH$_2$AlMe$_2$+H]$^+$, 177 (20), 159 (18), 57 (40) [*t*Bu]$^+$.

4.6. References

[1] a) Aresta M. *Carbon Dioxide as Chemical Feedstock;* WILEY-VCH Verlag GmbH & Co. KGaA: Weinheim, **2010**; b) see also the *ChemSusChem* special issue (Issue 9) on *Carbon Dioxide Recycling*, *ChemSusChem*. **2011**, *4*, 1177–1323.

[2] Tolman W. B. *Activation of Small Molecules;* WILEY-VCH Verlag GmbH & Co. KGaA: Weinheim, **2006**.

[3] Anastas P. T.; Warner J. C. *Green Chemistry Theory & Practice*; Oxford University Press: Oxford, **1998**.

[4] Reviews on FLPs: (a) Stephan D. W.; Erker G. *Angew. Chem. Int. Ed.* **2010**, *49*, 46–76; (b) Stephan D. W. *Dalton Trans.* **2009**, 3129–3136; c) Stephan D. W. *Org. Biomol. Chem.* **2008**, *6*, 1535–1539; d) Erker G. *C. R. Chimie* **2011,** *14*, 831–841; d) Stephan D. W. *Org. Biomol. Chem.* **2012**, *10*, 5740–5746; e) Stephan D. W. *Chem. Comm.* **2012**, *46*, 8526–8533.

[5] (a) Geier S. J.; Stephan D. W. *J. Am. Chem. Soc.* **2009**, *131*, 3476–3477; (b) Spies P.; Erker G.; Kehr G.; Bergander K.; Fröhlich R.; Grimme S.; Stephan D. W. *Chem. Comm.* **2007**, 5072–5074; (c) Welch G. C.; Cabrera L.; Chase P. A.; Hollink E.; Masuda J. D.; Wei P.; Stephan D. W. *Dalton Trans.* **2007**, 3407–3414; (d) Welch G. C.; Prieto R.; Dureen M. A.; Lough A. J.; Labeodan O. A.; Holtrichter-Rössmann T.; Stephan D. W. *Dalton Trans*. **2009**, 1559–1570; (e) Dureen M. A.; Stephan D. W. *J. Am. Chem. Soc.* **2009**, *131*, 8396–8397; (f) Ménard G.; Stephan D. W. *J. Am. Chem. Soc.* **2010**, *132*, 1796–1797; (g) Jiang C.; Blacque O.; Berke H. *Organometallics* **2010**, *30*, 2117–2124; (h) Wu D.; Jia D.; Liu L.; Zhang L.; Guo J. *J. Phys. Chem. A* **2010**, *114*, 11738–11745.

[6] (a) Mömming C. M.; Frömel S.; Kehr G.; Fröhlich R.; Grimme S.; Erker G. *J. Am. Chem. Soc.* **2009**, *131*, 12280–12289; (b) Mömming C. M.; Kehr G.; Fröhlich R.; Erker G. *Dalton Trans*. **2010**, *39*, 7556–7564; (c) Mömming C. M.; Kehr G.; Wibbeling B.; Fröhlich R.; Schirmer B.; Grimme S.; Erker G. *Angew. Chem. Int. Ed.* **2010**, *49*, 2414 –2417.

[7] Spies P.; Schwendemann S.; Lange S.; Kehr G.; Fröhlich R.; Erker G. *Angew. Chem. Int. Ed*. **2008**, *47*, 7543–7546.

[8] (a) Appelt C.; Westenberg H.: Bertini F.; Ehlers A. W.; Slootweg J. C.; Lammertsma K.; Uhl W. *Angew. Chem. Int. Ed.* **2011**, *50*, 3925–3928. (b) Appelt C.; Slootweg J. C.; Lammertsma K.; Uhl W. *Angew. Chem. Int. Ed.* **2012**, *51*, 5911–5914.

[9] For a methylene-bridged P/B-based frustrated Lewis pair, see: Bertini F.; Lyaskovskyy V.; Timmer B. J. J.; de Kanter F. J. J.; Lutz M.; Ehlers A. W.; Slootweg J. C.; Lammertsma K. *J. Am. Chem. Soc*. **2012**, *134*, 201–204.

[10] synthesis of tBu$_2$PCH$_2$Li: Eisenträger F.; Göthlich A.; Gruber I.; Heiss H.; Kiener C. A.; Krüger C.; Notheis J. U.; Rominger F.; Scherhag G.: Schultz M.; Straub B. F.; Vollanda M. A. O.; Hofmann P. *New J. Chem.* **2003**, *27*, 540–550.

[11] Roters S.; Appelt C.; Westenberg H.; Hepp A.; Slootweg J. C.; Lammertsma K.; Uhl W. *Dalton Trans.* DOI:10.1039/c2dt30080j

[12] Karsch H. H.; Appelt A.; Köhler F. H.; Müller G. *Organometallics* **1985**, *4*, 231–238.

[13] Fontaine F.G.; Zagarian D. *J. Am. Chem. Soc.* **2004**, *126*, 8786–8794.

[14] Thibault M. H.; Boudreau J.; Methiotte S.; Drouin F.; Sigouin O.; Michaud A.; Fontaine F. G.; Zagarian D. *Organometallics* **2007**, *26*, 3804–3815.

[15] Boudreau J.; Courtemanche M. A.; Fontaine F. G. *Chem. Commun*. **2011**, *47*, 11131–11133.

[16] (a) Zhao Y.; Truhlar D. G. *Acc. Chem. Res*. **2008**, *41*, 157–167; (b) Zhao Y.; Truhlar D. G. *Theor. Chem. Account* **2008**, *120*, 215–241; (c) Janesko B. G. *J. Chem. Theory Comput.* **2010**, *6*, 1825–1833. DFT calculations were carried out with Gaussian 09 (Revision A.02).

[17] The chair conformation was found to be ΔG = –3.7 kcal·mol^{-1} more stable than the twisted boat, see the Computational Section.

[18] We observed deviations in the computed relative energies within ±3 kcal·mol^{-1}; see Computational Section for additional details.

[19] The ^{13}C NMR resonance for the CO_2 carbon is in good agreement with those reported for similar aluminium dicarboxylates: Bethley C. E.; Aitken C. L.; Harlan C. J.; Koide Y.; Bott S. G.; Barron A. R. *Organometallics* **1997**, *16,* 329–341.

[20] Kwon H. J.; Kim H. W.; Rhee Y. M. *Chem. Eur. J*. **2011**, *17*, 6501–6507.

[21] a) Moebs-Sanchez S.; Bouhadir G.; Saffon N.; Maron L.; Bourissou D. *Chem. Commun.* **2008**, 3435–3437; b) Mömming C. M.; Kehr G.; Wibbeling B.; Fröhlich R.; Erker G. *Dalton Trans*. **2010**, 39, 7556–7564; c) Axenov K. V.; Mömming C. M.; Kehr G.; Fröhlich R.; Erker G. *Chem. Eur. J.* **2010**, *16*, 14069–14073.

[22] a) Stute A.; Kehr G.; Fröhlich R.; Erker G. *Chem. Commun*. **2011**, *47*, 4288–4290; b) Rosorius C.; Kehr G.: Fröhlich R.; Grimme S.; Erker G. *Organometallics* **2011**, *30*, 4211–4219.

[23] Gaussian 09, Revision A.02, Frisch M. J.; Trucks G. W.; Schlegel H. B.; Scuseria G. E.; Robb M. A.; Cheeseman J. R.; Scalmani G.; Barone V.; Mennucci B.; Petersson G. A.; Nakatsuji H.; Caricato M.; Li X.; Hratchian H. P.; Izmaylov A. F.; Bloino J.; Zheng G.; Sonnenberg J. L.; Hada M.; Ehara M.; Toyota K.; Fukuda R.; Hasegawa J.; Ishida M.; Nakajima T.; Honda Y.; Kitao O.; Nakai H.; Vreven T.; Montgomery J. A. Jr.; Peralta J. E.; Ogliaro F.; Bearpark M.; Heyd J. J.; Brothers E.; Kudin K. N.; Staroverov V. N.; Kobayashi R.; Normand J.; Raghavachari K.; Rendell A.; Burant J. C.; Iyengar S. S.; Tomasi J.; Cossi M.; Rega N.; Millam J. M.; Klene M.; Knox J. E.; Cross J. B.; Bakken V.; Adamo C.; Jaramillo J.; Gomperts R.; Stratmann R. E.; Yazyev O.; Austin A. J.; Cammi R.; Pomelli C.; Ochterski J. W.; Martin R. L.; Morokuma K.; Zakrzewski V. G.; Voth G. A.; Salvador P.; Dannenberg J. J.; Dapprich S.; Daniels A. D.; Farkas O.; Foresman J. B.; Ortiz J. V.; Cioslowski J.; Fox D. J. Gaussian, Inc., Wallingford CT, **2009**.